arXiv:1409.3474v1 [math.NA] 11 Sep 2014

An adaptive generalized multiscale discontinuous Galerkin method (GMsDGM) for high-contrast flow problems

Eric T. Chung*, Yalchin Efendiev† and Wing Tat Leung‡

September 12, 2014

Abstract

In this paper, we develop an adaptive Generalized Multiscale Discontinuous Galerkin Method (GMsDGM) for a class of high-contrast flow problems, and derive a-priori and a-posteriori error estimates for the method. Based on the a-posteriori error estimator, we develop an adaptive enrichment algorithm for our GMsDGM and prove its convergence. The adaptive enrichment algorithm gives an automatic way to enrich the approximation space in regions where the solution requires more basis functions, which are shown to perform well compared with a uniform enrichment. We also discuss an approach that adaptively selects multiscale basis functions by correlating the residual to multiscale basis functions (cf. [4]). The proposed error indicators are L_2-based and can be inexpensively computed which makes our approach efficient. Numerical results are presented that demonstrate the robustness of the proposed error indicators.

1 Introduction

Model reduction techniques are often required for solving challenging multiscale problems that have multiple scales and high contrast. Many of these model reduction techniques perform the discretization of the problem on a coarse grid where coarse grid size is much larger than the fine-grid discretization. The latter requires constructing reduced order models for the solution space on a coarse grid. Some of these techniques involve upscaled models (e.g., [13, 28]) or multiscale methods (e.g., [2, 5, 14, 18, 19, 20, 21, 6, 10, 7, 8]).

In this paper, we develop an adaptive Generalized Multiscale Discontinuous Galerkin Method (GMsDGM) for a class of high-contrast flow problems, and derive a-priori and a-posteriori error estimates for the method. We propose an adaptive enrichment algorithm for our GMsDGM based on the a-posteriori error estimator and prove its convergence. The enrichment is done using inexpensive L_2-based error indicators which allows adding more basis functions in an automatic way.

The Generalized Multiscale Finite Element Method (GMsFEM), introduced in [15], is a generalization of the classical multiscale finite element method ([22]) by systematically enriching the coarse spaces and taking into account small scale information and complex input spaces. While GMsFEM uses continuous Galerkin methods as coarse grid solvers, the GMsDGM considered in this paper is based on the interior penalty discontinuous Galerkin method as the coarse grid solver. The discontinuous Galerkin formulation has several key advantages in multiscale finite element methods (see [16]). The basis functions for the GMsDGM are totally decoupled across coarse element boundaries. In addition, the GMsDGM is constructed following the general framework on GMsFEM [15]. In particular, given a coarse grid partition of the computational domain, a snapshot space is defined for each coarse element. The snapshot space for a specific coarse element

*Department of Mathematics, The Chinese University of Hong Kong, Hong Kong SAR. This research is partially supported by the Hong Kong RGC General Research Fund (Project number: 400411).

†Department of Mathematics, Texas A&M University, College Station, TX; Numerical Porous Media SRI Center, King Abdullah University of Science and Technology (KAUST), Thuwal 23955-6900, Kingdom of Saudi Arabia

‡Department of Mathematics, Texas A&M University, College Station, TX.

contains all functions defined in the underlying fine grid. A space reduction is then performed to obtain a much smaller space by means of spectral decomposition. Our analysis shows that we need two spectral problems for the space reduction. More precisely, the snapshot space is decomposed into two components, which consists of harmonic extensions and functions that are vanishing on coarse element boundaries. Two separate spectral problems are used to compute reduced spaces. A-priori error estimate is derived showing that the error is inverse proportional to the first eigenvalue corresponding to the first eigenfunction that is not used in the construction of the reduced space. We remark that similar results are obtained for GMsFEM [18, 17].

It is evident that different coarse elements need different number of basis functions in order to obtain accurate representation of the solution. For example, in less heterogeneous regions, one needs fewer basis functions compared to the regions with more heterogeneities and high contrast. It is therefore another objective of the paper to consider adaptive enrichment of basis functions. We derive a-posteriori error estimate for the GMsDGM. By using the error indicator, we construct an adaptive enrichment algorithm and prove its convergence. One important feature of our adaptive enrichment algorithm is the ability to adaptively select basis functions in the space of harmonic extensions and the space of functions vanishing on coarse element boundaries. In addition, the error indicators are L_2-based, which can be computed efficiently. This is an advantage over the H^{-1}-based adaptive enrichment algorithm developed for GMsFEM [9]. We also present a procedure for removing basis functions. Our analysis is based on the idea in [3, 24, 9], and do not consider the error due to the fine-grid discretization of local problems and only study the errors due to the enrichment. In this regard, we assume that the error is largely due to coarse-grid discretization. The fine-grid discretization error can be considered in general (e.g., as in [1, 12]) and this will give an additional error estimator. We remark that there are many related activities in designing a-posteriori error estimates [11, 12, 1, 23, 25, 27] for global reduced models. The main difference is that our error estimators are based on special local eigenvalue problem and use the eigenstructure of the offline space. We also discuss an approach that adaptively selects multiscale basis functions from the offline space by selecting a basis with the most correlation to the local residual (cf. [4]).

The rest of the paper is organized in the following way. In the next section, we present the basic idea of GMsDGM. The method is then detailed and analyzed in Section 3. Then in Section 4, we elaborate the adaptive algorithm and state the main convergence results related to this algorithm. In Section 5, numerical results are illustrated to test the performance of this adaptive algorithm. The proofs of the main results are presented in Section 6.

2 Preliminaries

We will start this section with the problem settings and some notations. Let D be the computational domain consisting of a medium modeled by the function $\kappa(x)$. The high-contrast flow problem concerned in this paper is

$$-\operatorname{div}\big(\kappa(x)\,\nabla u\big) = f \quad \text{in} \quad D, \tag{1}$$

subject to the homogeneous Dirichlet boundary condition $u = g$ on ∂D. The main difficulty in numerically solving the above problem is that $\kappa(x)$ is highly heterogeneous with many scales and high contrast. We assume that $\kappa \geq 1$. In order to efficiently obtain an approximate solution to (1), we will need the notion of fine and coarse grids.

Consider a given triangulation $\mathcal{T}^H$ of the domain D with mesh size $H > 0$. We call $\mathcal{T}^H$ the coarse grid and H the coarse mesh size. Elements of $\mathcal{T}^H$ are called coarse grid blocks and we use N to denote the number of coarse grid blocks. The set of all coarse grid edges is denoted by $\mathcal{E}^H$. We also introduce a finer triangulation $\mathcal{T}^h$ of the computational domain D, obtained by a conforming refinement of the coarse grid $\mathcal{T}^H$. We call $\mathcal{T}^h$ the fine grid and $h > 0$ the fine mesh size. We remark that the use of the conforming refinement is only to simplify the discussion of the methodology and is not a restriction of the method.

Now we present the framework of GMsDGM. The methodology consists of two main ingredients, namely, the construction of local basis functions and the global coarse grid level coupling. For the local basis functions,

a snapshot space $V^{i,\text{snap}}$ is first constructed for each coarse grid block $K_i \in \mathcal{T}^H$. The snapshot space contains a large library of basis functions, which can be used to obtain a fine scale approximate solution to (1). A spectral problem is then solved in the snapshot space $V^{i,\text{snap}}$ and eigenfunctions corresponding to dominant modes are used as the final basis functions. The resulting space is called the local offline space $V^{i,\text{off}}$ for the i-th coarse grid block K_i. The global offline space V^{off} is then defined as the linear span of all these $V^{i,\text{off}}$, for $i = 1, 2, \cdots, N$. This global offline space V^{off} will be used as the approximation space of our discontinuous Galerkin method, which can be formulated as: find $u_H^{\text{DG}} \in V^{\text{off}}$ such that

$$a_{\text{DG}}(u_H^{\text{DG}}, v) = (f, v), \quad \forall v \in V^{\text{off}}, \tag{2}$$

where the bilinear form a_{DG} is defined as

$$a_{\text{DG}}(u, v) = a_H(u, v) - \sum_{E \in \mathcal{E}^H} \int_E \Big(\{\kappa \nabla u \cdot n_E\} [\![v]\!] + \{\kappa \nabla v \cdot n_E\} [\![u]\!] \Big) + \sum_{E \in \mathcal{E}^H} \frac{\gamma}{h} \int_E \overline{\kappa} [\![u]\!] [\![v]\!] \tag{3}$$

with

$$a_H(u, v) = \sum_{K \in \mathcal{T}_H} a_H^K(u, v), \quad a_H^K(u, v) = \int_K \kappa \nabla u \cdot \nabla v, \tag{4}$$

where $\gamma > 0$ is a penalty parameter, n_E is a fixed unit normal vector defined on the coarse edge $E \in \mathcal{E}^H$. Note that, in (3), the average and the jump operators are defined in the classical way. Specifically, consider an interior coarse edge $E \in \mathcal{E}^H$ and let K^+ and K^- be the two coarse grid blocks sharing the edge E. For a piecewise smooth function G, we define

$$\{G\} = \frac{1}{2}(G^+ + G^-), \qquad [\![G]\!] = G^+ - G^-, \qquad \text{on } E,$$

where $G^+ = G|_{K^+}$ and $G^- = G|_{K^-}$ and we assume that the normal vector n_E is pointing from K^+ to K^-. Moreover, on the edge E, we define $\overline{\kappa} = (\kappa_{K^+} + \kappa_{K^-})/2$ where $\kappa_{K^\pm}$ is the maximum value of κ over $K^\pm$. For a coarse edge E lying on the boundary ∂D, we define

$$\{G\} = [\![G]\!] = G, \quad \text{and} \quad \overline{\kappa} = \kappa_K \qquad \text{on } E,$$

where we always assume that n_E is pointing outside of D. We note that the DG coupling (2) is the classical interior penalty discontinuous Galerkin (IPDG) method [26] with our multiscale basis functions as the approximation space.

3 GMsDGM for high-contrast flow problems

In this section, we will give a detailed description of the method. We will first give the construction of the snapshot space, and then give the definitions of the local spectral problems for the construction of the offline space. Furthermore, a priori estimate of the method will be derived.

Let $K_i \in \mathcal{T}^H$ be a given coarse grid block. We will define two types of snapshot spaces. The first type of local snapshot space $V_1^{i,\text{snap}}$ for the coarse grid block K_i is defined as the linear span of all harmonic extensions. Specifically, given a function δ_k defined on ∂K_i, we find $\psi_k^{i,\text{snap}} \in V_h(K_i)$ by

$$\begin{aligned} \int_{K_i} \kappa \nabla \psi_k^{i,\text{snap}} \cdot \nabla v = 0, \quad \forall\, v \in V_h^0(K_i), \\ \psi_k^{i,\text{snap}} = \delta_k, \quad \text{on } \partial K_i, \end{aligned} \tag{5}$$

where $V_h(K_i)$ is the standard conforming piecewise linear finite element space with respect to the fine grid defined on K_i, $V_h^0(K_i)$ is the subspace of $V_h(K_i)$ containing functions vanishing on ∂K_i and δ_k is piecewise linear on ∂K_i with respect to the fine grid such that δ_k has the value one at the k-th fine grid node and

value zero at all the remaining fine grid nodes. The linear span of the above harmonic extensions is the local snapshot space $V_1^{i,\text{snap}}$, namely

$$V_1^{i,\text{snap}} = \text{span}\{\psi_k^{i,\text{snap}}, \quad k = 1, 2, \cdots, M^{i,\text{snap}}\},$$

where $M^{i,\text{snap}}$ is the number of basis functions in $V_1^{i,\text{snap}}$, which is also equal to the number of fine grid nodes on ∂K_i. The second type of local snapshot space $V_2^{i,\text{snap}}$ for the coarse grid block K_i is defined as $V_2^{i,\text{snap}} = V_h^0(K_i)$. It is easy to see that $V_h(K_i) = V_1^{i,\text{snap}} + V_2^{i,\text{snap}}$, namely the space $V_h(K_i)$ is decomposed as the sum of harmonic extensions and functions vanishing on the boundary ∂K_i. Moreover, the global snapshot space V_1^{snap} is defined so that any $v \in V_1^{\text{snap}}$ if $v|_{K_i} \in V_1^{i,\text{snap}}$. The space V_2^{snap} is defined similarly.

We will perform dimension reductions on the above snapshot spaces by the use of some carefully selected spectral problems. Based on our analysis to be presented in this section, we define the spectral problem for $V_1^{i,\text{snap}}$ as finding eigenpairs $(\phi_k^{(i)}, \lambda_{1,k}^{(i)})$, $k = 1, 2, \cdots, M^{i,\text{snap}}$, such that

$$\int_{K_i} \kappa \nabla \phi_k^{(i)} \cdot \nabla v = \frac{\lambda_{1,k}^{(i)}}{H} \int_{\partial K_i} \widetilde{\kappa} \phi_k^{(i)} v, \qquad \forall v \in V_1^{i,\text{snap}}, \tag{6}$$

where $\widetilde{\kappa}$ is the maximum of $\overline{\kappa}$ over all coarse edges $E \in \partial K_i$. Moreover, we assume that

$$\lambda_{1,1}^{(i)} < \lambda_{1,2}^{(i)} < \cdots < \lambda_{1,M^{i,\text{snap}}}^{(i)}.$$

For the space $V_2^{i,\text{snap}}$, we define the spectral problem as finding eigenpairs $(\xi_k^{(i)}, \lambda_{2,k}^{(i)})$, $k = 1, 2, \cdots$, such that

$$\int_{K_i} \kappa \nabla \xi_k^{(i)} \cdot \nabla v = \frac{\lambda_{2,k}^{(i)}}{H^2} \int_{K_i} \kappa \xi_k^{(i)} v, \qquad \forall v \in V_2^{i,\text{snap}}, \tag{7}$$

where we also assume that

$$\lambda_{2,1}^{(i)} < \lambda_{2,2}^{(i)} < \cdots$$

In the spectral problems (6) and (7), we will take respectively the first $l_{1,i}$ and $l_{2,i}$ eigenfunctions to form the offline space for the coarse grid block K_i. The local offline spaces are then defined as

$$V_1^{i,\text{off}} = \text{span}\{\phi_l^{(i)}, \quad l = 1, 2, \cdots, l_{1,i}\},$$
$$V_2^{i,\text{off}} = \text{span}\{\xi_l^{(i)}, \quad l = 1, 2, \cdots, l_{2,i}\}.$$

We define $V^{i,\text{off}} = V_1^{i,\text{off}} + V_2^{i,\text{off}}$. The global offline space V_1^{off} is defined so that the restriction of any function $v \in V_1^{\text{off}}$ on the coarse grid block K_i belongs to $V_1^{i,\text{off}}$. The definition for V_2^{off} is defined similarly. In addition, we define $V^{\text{off}} = V_1^{\text{off}} + V_2^{\text{off}}$. This space is used as the approximation space in (2).

Now we will analyze the method defined in (2). For any piecewise smooth function u, we define the DG-norm by

$$\|u\|_{\text{DG}}^2 = a_H(u, u) + \sum_{E \in \mathcal{E}_H} \frac{\gamma}{h} \int_E \overline{\kappa} [\![u]\!]^2 \, ds.$$

Let K be a coarse grid block and let $n_{\partial K}$ be the unit outward normal vector on ∂K. We denote $V_h(\partial K)$ by the restriction of the conforming space $V_h(K)$ on ∂K. The normal flux $\kappa \nabla u \cdot n_{\partial K}$ is understood as an element in $V_h(\partial K)$ and is defined by

$$\int_{\partial K} (\kappa \nabla u \cdot n_{\partial K}) \cdot v = \int_K \kappa \nabla u \cdot \nabla \widehat{v}, \quad v \in V^h(\partial K), \tag{8}$$

where $\widehat{v} \in V_h(K)$ is the harmonic extension of v in K. By the Cauchy-Schwarz inequality,

$$\int_{\partial K} (\kappa \nabla u \cdot n_{\partial K}) \cdot v \leq a_H^K(u, u)^{\frac{1}{2}} \, a_H^K(\widehat{v}, \widehat{v})^{\frac{1}{2}}.$$

By an inverse inequality and the fact that $\widehat{v}$ is the harmonic extension of v

$$a_H^K(\widehat{v},\widehat{v}) \le \kappa_K C_{\rm inv}^2 h^{-1} \int_{\partial K} |v|^2, \tag{9}$$

where we recall that κ_K is the maximum of κ over K and $C_{\rm inv} > 0$ is the constant from inverse inequality. Thus,

$$\int_{\partial K} (\kappa \nabla u \cdot n_{\partial K}) \cdot v \le \kappa_K^{\frac{1}{2}} C_{\rm inv} h^{-\frac{1}{2}} \|v\|_{L^2(\partial K)}\, a_H^K(u,u)^{\frac{1}{2}}.$$

This shows that

$$\int_{\partial K} |\kappa \nabla u \cdot n_{\partial K}|^2 \le \kappa_K C_{\rm inv}^2 h^{-1} a_H^K(u,u). \tag{10}$$

Our first step in the development of an a priori estimate is to establish the continuity and the coercivity of the bilinear form (3) with respect to the DG-norm.

Lemma 3.1. *Assume that the penalty parameter γ is chosen so that $\gamma > C_{\rm inv}^2$. The bilinear form a_{DG} defined in (3) is continuous and coercive, that is,*

$$a_{DG}(u,v) \le a_1 \|u\|_{DG}\, \|v\|_{DG}, \tag{11}$$
$$a_{DG}(u,u) \ge a_0 \|u\|_{DG}^2, \tag{12}$$

for all u, v, where $a_0 = 1 - C_{\rm inv}\gamma^{-\frac{1}{2}} > 0$ and $a_1 = 1 + C_{\rm inv}\gamma^{-\frac{1}{2}}$.

Proof. By the definition of $a_{\rm DG}$, we have

$$a_{\rm DG}(u,v) = a_H(u,v) - \sum_{E\in\mathcal{E}^H} \int_E \Big(\{\kappa \nabla u \cdot n_E\} [\![v]\!] + \{\kappa \nabla v \cdot n_E\} [\![u]\!] \Big) + \sum_{E\in\mathcal{E}^H} \frac{\gamma}{h} \int_E \overline{\kappa} [\![u]\!] [\![v]\!].$$

Notice that

$$a_H(u,v) + \sum_{E\in\mathcal{E}^H} \frac{\gamma}{h} \int_E \overline{\kappa} [\![u]\!] \cdot [\![v]\!] \le \|u\|_{\rm DG}\, \|v\|_{\rm DG}.$$

For an interior coarse edge $E \in \mathcal{E}^H$, we let $K^+, K^- \in \mathcal{T}^H$ be the two coarse grid blocks having the edge E. By the Cauchy-Schwarz inequality, we have

$$\int_E \{\kappa \nabla u \cdot n_E\} \cdot [\![v]\!] \le \Big(h \int_E \{\kappa \nabla u \cdot n_E\}^2 (\overline{\kappa})^{-1} \Big)^{\frac{1}{2}} \Big(\frac{1}{h} \int_E \overline{\kappa} [\![v]\!]^2 \Big)^{\frac{1}{2}}. \tag{13}$$

Notice that

$$h \int_E \{\kappa \nabla u \cdot n_E\}^2 (\overline{\kappa})^{-1} \le h \Big(\int_E (\kappa^+ \nabla u^+ \cdot n_E)^2 (\kappa_{K^+})^{-1} + \int_E (\kappa^- \nabla u^- \cdot n_E)^2 (\kappa_{K^-})^{-1} \Big)$$

where $u^\pm = u|_{K^\pm}$, $\kappa^\pm = \kappa|_{K^\pm}$. So, summing the above over all E and by (10), we have

$$h \sum_{E\in\mathcal{E}^H} \int_E \{\kappa \nabla u \cdot n_E\}^2 (\overline{\kappa})^{-1} \le h \sum_{K\in\mathcal{T}_H} \int_{\partial K} (\kappa \nabla u \cdot n_{\partial K})^2 (\kappa_K)^{-1} \le C_{\rm inv}^2 a_H(u,u).$$

Thus we have

$$\sum_{E\in\mathcal{E}^H} \int_E \{\kappa \nabla u \cdot n_E\} [\![v]\!] \le C_{\rm inv} a_H(u,u)^{\frac{1}{2}} \Big(\sum_{E\in\mathcal{E}^H} \frac{1}{h} \int_E \overline{\kappa} [\![v]\!]^2\, ds \Big)^{\frac{1}{2}}. \tag{14}$$

Similarly, we have

$$\sum_{E\in\mathcal{E}^H} \int_E \{\kappa \nabla v \cdot n_E\} [\![u]\!] \le C_{\rm inv} a_H(v,v)^{\frac{1}{2}} \Big(\sum_{E\in\mathcal{E}^H} \frac{1}{h} \int_E \overline{\kappa} [\![u]\!]^2\, ds \Big)^{\frac{1}{2}}.$$

Summing the above two inequalities, we have

$$\sum_{E\in\mathcal{E}^H}\int_E\Big(\{\kappa\nabla u\cdot n_E\}[\![v]\!]+\{\kappa\nabla v\cdot n_E\}[\![u]\!]\Big)\le C_{\rm inv}\gamma^{-\frac{1}{2}}\|u\|_{\rm DG}\,\|v\|_{\rm DG}. \tag{15}$$

This proves the continuity (11).

For the coercivity (12), we have

$$a_{\rm DG}(u,u)=\|u\|_{\rm DG}^2-\sum_{E\in\mathcal{E}^H}\int_E\Big(\{\kappa\nabla u\cdot n_E\}\cdot[\![u]\!]+\{\kappa\nabla u\cdot n_E\}\cdot[\![u]\!]\Big).$$

By (15), we have

$$a_{\rm DG}(u,u)\ge(1-C_{\rm inv}\gamma^{-\frac{1}{2}})\|u\|_{\rm DG}^2,$$

which gives the desired result.

□

In the following, we will prove an a priori estimate of the method (2). First, we let

$$V_{\rm DG}^h=\{v\in L^2(D)\,:\,v|_K\in V^h(K)\}.$$

Let $u_h\in V_{\rm DG}^h$ be the fine grid solution which satisfies

$$a_{\rm DG}(u_h,v)=(f,v),\quad\forall v\in V_{\rm DG}^h. \tag{16}$$

It is well-known that u_h converges to the exact solution u in the DG-norm as the fine mesh size $h\to 0$. Next, we define a projection $u_1\in V_1^{\rm snap}$ of u_h in the snapshot space by the following construction. For each coarse grid block K_i, the restriction of u_1 on K_i is defined as the harmonic extension of u_h, that is,

$$\begin{aligned}\int_{K_i}\kappa\nabla u_1\cdot\nabla v=0,\qquad&\forall\, v\in V_h^0(K_i)\\ u_1=u_h,\quad&\text{on }\ \partial K_i.\end{aligned} \tag{17}$$

The following theorem gives an a priori estimate for the GMsDGM (2).

Theorem 3.2. *Let $u_h\in V_{DG}^h$ be the fine grid solution defined in (16) and u_H be the GMsDGM solution defined in (2). Then we have*

$$\begin{aligned}\|u_h-u_H\|_{DG}^2\le C\Big(&\sum_{i=1}^N\frac{H}{\widetilde{\kappa}\lambda_{1,l_{1,i}+1}^{(i)}}(1+\frac{\gamma H}{h\lambda_{1,l_{1,i}+1}^{(i)}})\int_{\partial K_i}(\kappa\nabla u_1\cdot n_{\partial K})^2+\sum_{K\in\mathcal{T}_H}\frac{H^2}{\lambda_{2,l_{2,i}+1}^{(i)}}\|f\|_{L^2(K)}^2\\&+C_{\rm inv}^2\sum_{E\in\mathcal{E}^H}\frac{1}{h}\int_E\overline{\kappa}[\![u_h]\!]^2\Big),\end{aligned}$$

where u_1 is defined in (17).

Proof. First, we write $u_h=u_1+u_2$ where $u_2=u-u_1$. Notice that, on each coarse grid block K_i, the functions u_1 and u_2 can be represented by

$$u_1=\sum_{l=1}^{M_i}c_l\phi_l^{(i)}\quad\text{and}\quad u_2=\sum_{l\ge1}d_l\xi_l^{(i)} \tag{18}$$

where $M_i=M^{i,\rm snap}$ and we assume that the functions $\phi_l^{(i)}$ and $\xi_l^{(i)}$ are normalized so that

$$\int_{\partial K_i}\overline{\kappa}(\phi_l^{(i)})^2=1\quad\text{and}\quad\int_{K_i}\kappa(\xi_l^{(i)})^2=1.$$

Notice that, the functions u_1 and u_2 belong to the snapshot spaces V_1^{snap} and V_2^{snap} respectively. We will need two functions $\widehat{u}_1$ and $\widehat{u}_2$, which belong to the offline spaces V_1^{off} and V_2^{off} respectively. These functions are defined by

$$\widehat{u}_1 = \sum_{l=1}^{l_{1.i}} c_l \phi_l^{(i)} \quad \text{and} \quad \widehat{u}_2 = \sum_{l=1}^{l_{2.i}} d_l \xi_l^{(i)} \qquad \text{on } K_i.$$

We remark that $\widehat{u}_1$ and $\widehat{u}_2$ are the truncation of u_1 and u_2 up to the eigenfunctions selected to form the offline space.

Next, we will find an estimate of $\|u_1 - \widehat{u}_1\|_{\text{DG}}$. Let $K_i \in \mathcal{T}^H$ be a given coarse grid block. Recall that the spectral problem to form $V_1^{i,\text{off}}$ is

$$\int_{K_i} \kappa \nabla \phi_k^{(i)} \cdot \nabla v = \frac{\lambda_{1,k}^{(i)}}{H} \int_{\partial K_i} \widetilde{\kappa} \phi_k^{(i)} v, \qquad \forall v \in V_1^{i,\text{snap}}.$$

By the definition of the flux defined in (8), the above spectral problem can be represented as

$$\int_{\partial K_i} (\kappa \nabla \phi_k^{(i)} \cdot n_{\partial K_i}) v \, ds = \frac{\lambda_{1,k}^{(i)}}{H} \int_{\partial K_i} \widetilde{\kappa} \phi_k^{(i)} v.$$

By the definition of the DG-norm, the error $\|u_1 - \widehat{u}_1\|_{\text{DG}}$ can be estimated by

$$\|\widehat{u}_1 - u_1\|_{\text{DG}}^2 \leq \sum_{i=1}^{N} \Big(\int_{K_i} \kappa |\nabla(\widehat{u}_1 - u_1)|^2 + \frac{\gamma}{h} \int_{\partial K_i} \widetilde{\kappa} (\widehat{u}_1 - u_1)^2 \Big).$$

Note that, by (18), we have

$$\int_{K_i} \kappa |\nabla(\widehat{u}_1 - u_1)|^2 = \sum_{l=l_{1,i}+1}^{M_i} \frac{\lambda_{1,l}^{(i)}}{H} c_l^2 \leq \frac{H}{\lambda_{1,l_{1,i}+1}^{(i)}} \sum_{l=l_{1,i}+1}^{M_i} (\frac{\lambda_{1,l}^{(i)}}{H})^2 c_l^2$$

and

$$\frac{1}{h} \int_{\partial K_i} \widetilde{\kappa} (\widehat{u}_1 - u_1))^2 = \frac{1}{h} \sum_{l=l_{1,i}+1}^{M_i} c_l^2 \leq \frac{H^2}{h(\lambda_{1,l_{1,i}+1}^{(i)})^2} \sum_{l=l_{1,i}+1}^{M_i} (\frac{\lambda_{1,l}^{(i)}}{H})^2 c_l^2.$$

Furthermore,

$$\sum_{l=l_{1,i}+1}^{M_i} (\frac{\lambda_{1,l}^{(i)}}{H})^2 c_l^2 \leq \sum_{l=1}^{M_i} (\frac{\lambda_{1,l}^{(i)}}{H})^2 c_l^2 = (\widetilde{\kappa})^{-1} \int_{\partial K_i} (\kappa \nabla u_1 \cdot n_{\partial K_i})^2.$$

Consequently, we obtain the following bound

$$\|u_1 - \widehat{u}_1\|_{\text{DG}}^2 \leq \sum_{i=1}^{N} \frac{H}{\widetilde{\kappa} \lambda_{1,l_{1,i}+1}^{(i)}} (1 + \frac{\gamma H}{h \lambda_{1,l_{1,i}+1}^{(i)}}) \int_{\partial K_i} (\kappa \nabla u_1 \cdot n_{\partial K})^2.$$

Next, we will find an estimate of $\|u_2 - \widehat{u}_2\|_{\text{DG}}$. By definition of the bilinear form a_{DG},

$$a_{DG}(u_2, v) = -a_{DG}(u_1, v) + (f, v) = \sum_{E \in \mathcal{E}^H} \int_E \Big(\{\kappa \nabla v \cdot n_E\} [\![u_1]\!] \Big) + (f, v)$$

which holds for any $v \in V_2^{\text{snap}}$. In addition, by the fact that any function in V_2^{snap} is zero on boundaries of coarse grid blocks, we have

$$\|u_2 - \widehat{u}_2\|_{\text{DG}}^2 = a_{DG}(u_2 - \widehat{u}_2, u_2 - \widehat{u}_2) = a_{DG}(u_2, u_2 - \widehat{u}_2),$$

where the last equality follows from the fact that the eigenfunctions of (7) are κ-orthogonal on every coarse grid block. Therefore we have

$$\|u_2-\widehat{u}_2\|^2_{\mathrm{DG}}=\sum_{E\in\mathcal{E}^H}\int_E\Big(\{\kappa\nabla(u_2-\widehat{u}_2)\cdot n_E\}[\![u_1]\!]\Big)+(f,u_2-\widehat{u}_2). \tag{19}$$

The second term on the right hand side of (19) can be estimated as

$$(f,u_2-\widehat{u}_2)\leq\sum_{K\in\mathcal{T}^H}\|f\|_{L^2(K)}\|\kappa^{\frac{1}{2}}(u_2-\widehat{u}_2)\|_{L^2(K)}.$$

By (7), for every $K_i\in\mathcal{T}^H$, we have

$$\int_{K_i}\kappa|(u_2-\widehat{u}_2)|^2=\sum_{l\geq l_{2,i}+1}d_l^2\leq\Big(\frac{H^2}{\lambda^{(i)}_{2,l_{2,i}+1}}\Big)\sum_{l=l_{2,i}+1}\frac{\lambda^{(i)}_{2,l}}{H^2}d_l^2=\frac{H^2}{\lambda^{(i)}_{2,l_{2,i}+1}}\int_{K_i}\kappa|\nabla(u_2-\widehat{u}_2)|^2.$$

For the first term on the right hand side of (19), we use inequality (14) to conclude that

$$\sum_{E\in\mathcal{E}^H}\int_E\Big(\{\kappa\nabla(u_2-\widehat{u}_2)\cdot n_E\}[\![u_1]\!]\Big)\leq C_{\mathrm{inv}}\gamma^{-\frac{1}{2}}\|u_2-\widehat{u}_2\|_{\mathrm{DG}}\Big(\sum_{E\in\mathcal{E}^H}\frac{\gamma}{h}\int_E\overline{\kappa}[\![u_1]\!]^2\Big)^{\frac{1}{2}}.$$

Consequently, from (19) and the fact that $[\![u_1]\!]=[\![u_h]\!]$ for all coarse edges, we obtain the following bound

$$\|u_2-\widehat{u}_2\|^2_{\mathrm{DG}}\leq C\Big(C^2_{\mathrm{inv}}\sum_{E\in\mathcal{E}^H}\frac{1}{h}\int_E\overline{\kappa}[\![u_h]\!]^2+\sum_{K\in\mathcal{T}_H}\frac{H^2}{\lambda^{(i)}_{2,l_{2,i}+1}}\|f\|^2_{L^2(K)}\Big).$$

Finally, we will prove the required error bound. By coercivity,

$$\begin{aligned}a_0\|\widehat{u}_1+\widehat{u}_2-u_H\|^2_{\mathrm{DG}}&\leq a_{\mathrm{DG}}(\widehat{u}_1+\widehat{u}_2-u_H,\widehat{u}_1+\widehat{u}_2-u_H)\\&=a_{\mathrm{DG}}(\widehat{u}_1+\widehat{u}_2-u_H,\widehat{u}_1+\widehat{u}_2-u_h)+a_{\mathrm{DG}}(\widehat{u}_1+\widehat{u}_2-u_H,u_h-u_H).\end{aligned}$$

Note that $a_{\mathrm{DG}}(\widehat{u}_1+\widehat{u}_2-u_H,u_h-u_H)=0$ since $\widehat{u}_1+\widehat{u}_2-u_H\in V^{\mathrm{off}}$. Using the above results,

$$\begin{aligned}&\|\widehat{u}_1+\widehat{u}_2-u_H\|^2_{\mathrm{DG}}\\&\leq C\Big(\sum_{i=1}^N\frac{H}{\widetilde{\kappa}\lambda^{(i)}_{1,l_{1,i}+1}}(1+\frac{\gamma H}{h\lambda^{(i)}_{1,l_{1,i}+1}})\int_{\partial K_i}(\kappa\nabla u_1\cdot n_{\partial K})^2+\sum_{K\in\mathcal{T}_H}\frac{H^2}{\lambda^{(i)}_{2,l_{2,i}+1}}\|f\|^2_{L^2(K)}+C^2_{\mathrm{inv}}\sum_{E\in\mathcal{E}^H}\frac{1}{h}\int_E\overline{\kappa}[\![u_h]\!]^2\Big).\end{aligned}$$

The desired bound is then obtained by the triangle inequality

$$\|u_h-u_H\|_{\mathrm{DG}}\leq\|u_h-\widehat{u}\|_{\mathrm{DG}}+\|\widehat{u}-u_H\|_{\mathrm{DG}},$$

where $\widehat{u}=\widehat{u}_1+\widehat{u}_2$. This completes the proof.

□

We remark that, the term

$$\sum_{i=1}^N\frac{H}{\widetilde{\kappa}\lambda^{(i)}_{1,l_{1,i}+1}}(1+\frac{\gamma H}{h\lambda^{(i)}_{1,l_{1,i}+1}})\int_{\partial K_i}(\kappa\nabla u_1\cdot n_{\partial K})^2 \tag{20}$$

corresponds to the error for the space V_1^{off} and the term

$$\sum_{K\in\mathcal{T}_H}\frac{H^2}{\lambda^{(i)}_{2,l_{2,i}+1}}\|f\|^2_{L^2(K)}$$

corresponds to the error for the space V_2^{off}. Moreover, the term

$$C_{\text{inv}}^2 \sum_{E\in\mathcal{E}^H} \frac{1}{h}\int_E \overline{\kappa}[\![u_h]\!]^2$$

is the error in the fine grid solution u_h. This is the irreducible error, and an estimate of this can be derived following standard DG frameworks.

h	Λ_K^{snap}
1/48	1.0021e+03
1/96	1.0193e+03
1/192	1.3094e+03

h	Λ_K^{snap}
1/48	7.7650e+05
1/96	1.6569e+06
1/192	3.3254e+06

Table 1: Left: oversampling basis, Right: no-oversampling basis

Remark 3.3. *It is important to note that one can also replace (9) by*

$$a_H^K(\widehat{v},\widehat{v}) \leq \Lambda_K^{snap}\widetilde{\kappa}\int_{\partial K}|v|^2, \tag{21}$$

where Λ_K^{snap} is the largest eigenvalue for the spectral problem (6). Therefore, (10) can be replaced by

$$\int_{\partial K}|\kappa\nabla u\cdot n_{\partial K}|^2 \leq \Lambda_K^{snap}\widetilde{\kappa}\, a_H^K(u,u).$$

By following the above steps, we see that one can choose γ in (20) so that

$$\gamma > C_\kappa h \max_{K\subset\mathcal{T}^H}\Lambda_K^{snap}$$

where the constant C_κ is defined as

$$C_\kappa = \max_{K\subset\mathcal{T}^H}\frac{\max_{E\subset\partial K}\overline{\kappa}}{\min_{E\subset\partial K}\overline{\kappa}}.$$

We remark that this constant C_κ is order one if we assume that every coarse element has a high contrast region.

One can take smaller values of γ if oversampling is used (oversampling method is discussed in Section 5). The main idea of the oversampling is to choose larger regions for computing snapshot vectors. For every coarse block K_i, we choose an enlarged region K_i^+, and find oversampling snapshot functions $\psi_k^{i,over}$ by solving (32). We have performed numerical experiments and computed Λ_K^{snap} with and without oversampling. Denote $\Lambda_{K^+}^{snap}$ to be the largest eigenvalue corresponding to the oversampled problem. In our numerical results (see Table 1), we have removed linearly dependent snapshot vectors with respect to the inner product corresponding to $\int_{\partial K}|v|^2$ before computing the largest eigenvalue. Our numerical results show that one can have about three orders of magnitude smaller value for $\Lambda_{K^+}^{snap}$ compared to Λ_K^{snap}. Moreover, our numerical results show a weak h-dependence for $\Lambda_{K^+}^{snap}$ as we decrease h, while Λ_K^{snap} behaves as h^{-1} (when no-oversampling is used).

Our error analysis holds when oversampling snapshot space is used. The term in (20) will become

$$\sum_{i=1}^N \frac{H}{\widetilde{\kappa}\lambda_{1,l_{1,i}+1}^{(i)}}\Big(1+\frac{\alpha C_\kappa \max_{K\subset\mathcal{T}^H}\Lambda_{K^+}^{snap}H}{\lambda_{1,l_{1,i}+1}^{(i)}}\Big)\int_{\partial K_i}(\kappa\nabla u_1\cdot n_{\partial K})^2 \tag{22}$$

when $\gamma = \alpha C_\kappa h\max_{K\subset\mathcal{T}^H}\Lambda_{K^+}^{snap}$. If $\Lambda_{K^+}^{snap}$ is a weak function of h, e.g., if it is bounded with respect to h, then the terms involving $\Lambda_{K^+}^{snap}$ doesnt influence the error and the error is dominated by the first term. We emphasize that our discussions in this Remark are based on our numerical studies and their analytical studies are difficult because it requires interior estimates for solutions. We plan to study them in future.

4 A-posteriori error estimate and adaptive enrichment

In this section, we will derive an a-posteriori error indicator for the error $u_h - u_H$ in energy norm. We will then use the error indicator to develop an adaptive enrichment algorithm. The a-posteriori error indicator gives an estimate of the local error on the coarse grid blocks K_i, and we can then add basis functions to improve the solution. Our indicator consists of two components, which correspond to the errors made in the spaces V_1^{snap} and V_2^{snap}. By using the indicator, one can determine adaptively which space has to be enriched. This section is devoted to the description of the a-posteriori error indicator and the corresponding adaptive enrichment algorithm. The convergence analysis of the method will be given in the Section 6.

Recall that V_{DG}^h is the fine scale DG finite element space, and the fine scale solution u_h satisfies

$$a_{\text{DG}}(u_h, v) = (f, v) \quad \text{for all } \ v \in V_{\text{DG}}^h. \tag{23}$$

Moreover, the GMsDGM solution u_H satisfies

$$a_{\text{DG}}(u_H, v) = (f, v) \quad \text{for all } \ v \in V^{\text{off}}. \tag{24}$$

We remark that $V^{\text{off}} \subset V_{\text{DG}}^h$. Next we will give the definitions of the residuals.

Definitions of residuals:

Let K_i be a given coarse grid block. We will define two residuals corresponding to the two types of snapshot spaces. First, on the space $V_1^{i,\text{snap}}$, we define the following linear functional

$$R_{1,i}(v) = \int_{K_i} fv - a_{\text{DG}}(u_H, v), \quad v \in V_1^{i,\text{snap}}. \tag{25}$$

Similarly, on the space $V_2^{i,\text{snap}}$, we define the following linear functional

$$R_{2,i}(v) = \int_{K_i} fv - a_{\text{DG}}(u_H, v), \quad v \in V_2^{i,\text{snap}}. \tag{26}$$

These residuals measure how well the solution u_H satisfies the fine-scale equation (23). Furthermore, on the snapshot spaces $V_1^{i,\text{snap}}$ and $V_2^{i,\text{snap}}$, we define the following norms

$$\|v\|^2_{V_1(K_i)} = H^{-1} \int_{\partial K_i} \widetilde{\kappa} v^2 \quad \text{and} \quad \|v\|^2_{V_2(K_i)} = H^{-2} \int_{K_i} \kappa v^2 \tag{27}$$

respectively. The norms of the linear functionals $R_{1,i}$ and $R_{2,i}$ are defined in the standard way, namely

$$\|R_{1,i}\| = \sup_{v \in V_1^{i,\text{snap}}} \frac{|R_{1,i}(v)|}{\|v\|_{V_1(K_i)}} \quad \text{and} \quad \|R_{2,i}\| = \sup_{v \in V_2^{i,\text{snap}}} \frac{|R_{2,i}(v)|}{\|v\|_{V_2(K_i)}}. \tag{28}$$

The norms $\|R_{1,i}\|$ and $\|R_{2,i}\|$ give estimates on the sizes of fine-scale residual errors with respect to the spaces $V_1^{i,\text{snap}}$ and $V_2^{i,\text{snap}}$.

We recall that, for each coarse grid block K_i, the eigenfunctions of the spectral problem (6) corresponding to the eigenvalues $\lambda_{1,1}^{(i)}, \cdots, \lambda_{1,l_{1,i}}^{(i)}$ and the eigenfunctions of the spectral problem (7) corresponding to the eigenvalues $\lambda_{2,1}^{(i)}, \cdots, \lambda_{2,l_{2,i}}^{(i)}$ are used in the construction of V^{off}. In addition, the energy error in this section and Section 6 is measured by $\|u\|_a^2 = a_{\text{DG}}(u, u)$, which is equivalent to the DG norm.

In Section 6, we will prove the following theorem, and we see that the norms $\|R_{j,i}\|$ give indications on the size of the energy norm error $\|u_h - u_H\|_a$.

Theorem 4.1. *Let u_h and u_H be the solutions of* (23) *and* (24) *respectively. Then*

$$\|u_h - u_H\|_a^2 \quad \leq \quad C_{err} \sum_{i=1}^{N} \sum_{j=1}^{2} \|R_{j,i}\|^2 (\lambda_{j,l_{j,i}+1}^{(i)})^{-1}. \tag{29}$$

where C_{err} is a uniform constant.

We will now present the adaptive enrichment algorithm. We use $m \geq 1$ to represent the enrichment level, $V^{\text{off}}(m)$ to represent the solution space at level m and u_H^m to represent the GMsDGM solution at the enrichment level m. For each coarse grid block K_i, we use $l_{j,i}^m$ to represent the number of eigenfunctions in $V_j^{i,\text{off}}$ used at the enrichment level m for the coarse region K_i. Assume that the initial offline space $V^{\text{off}}(0)$ is given.

Adaptive enrichment algorithm: Choose $0 < \theta < 1$. For each $m = 0, 1, \cdots$,

1. Step 1: Find the solution in the current space. That is, find $u_H^m \in V^{\text{off}}(m)$ such that

$$a_{\text{DG}}(u_H^m, v) = (f, v) \quad \text{for all } \ v \in V^{\text{off}}(m). \tag{30}$$

2. Step 2: Compute the local residuals. For each coarse grid block K_i, we compute

$$\eta_{j,i}^2 = \|R_{j,i}\|^2 (\lambda_{j,l_{j,i}^m+1}^{(i)})^{-1}, \quad j = 1, 2.$$

   Then we re-enumerate the above $2N$ residuals in the decreasing order, that is, $\eta_1^2 \geq \eta_2^2 \geq \cdots \geq \eta_{2N}^2$, where we adopted single index notations.

3. Step 3: Find the coarse grid blocks and spaces where enrichment is needed. We choose the smallest integer k such that

$$\theta \sum_{J=1}^{2N} \eta_J^2 \leq \sum_{J=1}^{k} \eta_J^2. \tag{31}$$

4. Step 4: Enrich the space. For each $J = 1, 2, \cdots, k$, we add basis function in $V_j^{i,\text{off}}$ according to the following rule. Let s be the smallest positive integer such that $\lambda_{j,l_{j,i}^m+s+1}^{(i)}$ is large enough (see the proof of Theorem 4.2) compared with $\lambda_{j,l_{j,i}^m+1}^{(i)}$. Then we include the eigenfunctions in the construction of the basis functions. The resulting space is denoted as $V^{\text{off}}(m+1)$.

We remark that the choice of s above will ensure the convergence of the enrichment algorithm, and in practice, the value of s is easy to obtain. Moreover, contrary to classical adaptive refinement methods, the total number of basis functions that we can add is bounded by the dimension of the snapshot space. Thus, the condition (31) can be modified as follows. We choose the smallest integer k such that

$$\theta \sum_{J=1}^{2N} \eta_J^2 \leq \sum_{J \in I} \eta_J^2,$$

where the index set I is a subset of $\{1, 2, \cdots, k\}$.

Finally, we state the convergence theorem.

Theorem 4.2. *There are positive constants δ, ρ and L_m such that the following contracting property holds*

$$\|u - u_H^{m+1}\|_a^2 + \frac{1}{\delta L_{m+1}} \sum_{J=1}^{2N} (S_J^{m+1})^2 \leq \varepsilon \Big(\|u - u_H^m\|_a^2 + \frac{1}{\delta L_m} \sum_{J=1}^{N} (S_J^m)^2 \Big).$$

Note that $0 < \varepsilon < 1$ and

$$\varepsilon = 1 - \frac{\theta^2 (1 - \rho L_m / L_{m+1})}{\theta^2 + C_{err} \delta L_m}.$$

We remark that the precise definitions of S_J^m as well as the constants δ, ρ and L_m are given in Section 6.

5 Numerical Results

In this section, we will present some numerical examples to demonstrate the performance of the adaptive enrichment algorithm. The domain Ω is taken as the unit square $[0,1]^2$ and is divided into 16×16 coarse blocks consisting of uniform squares. Each coarse block is then divided into 32×32 fine blocks consisting of uniform squares. Consequently, the whole domain is partitioned by a 512×512 fine grid blocks. We will use the following error quantities to compare the accuracy of our algorithm

$$e_2 = \frac{\|u_H - u_h\|_{L^2(\Omega)}}{\|u_h\|_{L^2(\Omega)}},\ e_a = \frac{\sqrt{a_{\mathrm{DG}}(u_H - u_h, u_H - u_h)}}{\sqrt{a_{\mathrm{DG}}(u_h, u_h)}}$$

$$e_2^{\mathrm{snap}} = \frac{\|u_H - u_{\mathrm{snap}}\|_{L^2(\Omega)}}{\|u_{\mathrm{snap}}\|_{L^2(\Omega)}},\ e_a^{\mathrm{snap}} = \frac{\sqrt{a_{\mathrm{DG}}(u_H - u_{\mathrm{snap}}, u_H - u_{\mathrm{snap}})}}{\sqrt{a_{\mathrm{DG}}(u_{\mathrm{snap}}, u_{\mathrm{snap}})}}$$

where u_H and u_h are the GMsDGM and the fine grid solutions respectively. Moreover, u_{snap} is the snapshot solution obtained by using all snapshot functions generated by an oversampling strategy, see below.

We consider the permeability field κ which is shown in Figure 1. The boundary condition is set to be bi-linear, $g = x_1 x_2$. We will consider two examples with two different source functions f. We will compare the result of V_1 enrichment, $V_1 - V_2$ enrichment, oversampling basis enrichment, uniform enrichment and the exact indicator enrichment. The following gives the details of these enrichments.

- V_1 **enrichment**: We use the error indicator, $\eta_{1,i}^2$ to perform the adaptive algorithm by enriching the basis functions in V_1 space only, that is, basis functions obtained by the first spectral problem (6). We use 4 basis functions from (6) and zero basis function from (7) in the initial step.

- $V_1 - V_2$ **enrichment**: We use both the error indicators, $\eta_{1,i}^2, \eta_{2,i}^2$ to perform the adaptive algorithm by enriching the basis functions in both V_1 and V_2 spaces, that is, basis functions from both spectral problems (6) and (7). We use 4 basis functions from (6) and zero basis function from (7) in the initial step.

- **Oversampling enrichment:** For every coarse block K_i, we choose an enlarged region K_i^+ (in the examples presented below, we enlarge the coarse block in each direction by a length H, that is K_i^+ is a 3×3 coarse blocks with K_i at the center). Then we find oversampling snapshot functions $\psi_k^{i,\mathrm{over}} \in V_h(K_i^+)$ by solving

$$\begin{aligned} \int_{K_i} \kappa \nabla \psi_k^{i,\mathrm{over}} \cdot \nabla v = 0, \quad \forall\ v \in V_h^0(K_i^+), \\ \psi_k^{i,\mathrm{over}} = \delta_k, \quad \text{on } \partial K_i^+. \end{aligned} \tag{32}$$

  The linear span of these snapshot functions is called $V^{i,\mathrm{over}}$. Then we choose 40 dominant oversampling basis functions by POD method. Specifically, we solve the following eigenvalue problem

$$\int_{K_i} \psi_k^{i,\mathrm{over}} v = \lambda_k^i \int_{\partial K_i^+} \psi_k^{i,\mathrm{over}} v, \quad \forall v \in V^{i,\mathrm{over}}.$$

  and choose the first 40 eigenfunctions with largest eigenvalues. Then we use these 40 functions as boundary conditions in (5) and repeat the remaining construction of the offline space.

- **Uniform enrichment**: We enrich the basis functions in V_1 space uniformly with 4 basis functions from the V_1 space in the initial step.

- **The exact indicator enrichment**: We use the exact error as the error indicator to perform the adaptive algorithm by enriching the basis functions in V_1 space only with 4 basis functions in the space V_1 in the initial step. Here, the exact error is defined as $\|u - u_H\|_a$.

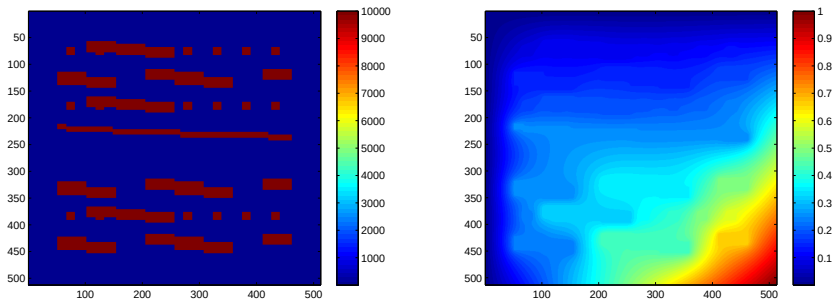

Figure 1: Left: Permeability field κ. Right: Fine grid solution with $f = 1$.

Example 1

In our first example, we take the source function $f = 1$. The fine grid solution is shown in Figure 1. In Table 2 and Table 3, we present the convergence history of our algorithm for enriching in V_1 space only, enriching in both V_1 and V_2 spaces and enriching by the oversampling basis functions. We remark that, in the presentation of our results, DOF means the total number of basis functions used in the whole domain. We see from Table 2 that the behaviour of enriching in V_1 space only and enriching in both V_1 and V_2 spaces are similar. The is due to the fact that the source function f is a constant function, and the space V_2 will not help to improve the solution. This is in consistent with classical theory that basis functions obtained by harmonic extensions are good enough to approximate the solution. In Table 3, the convergence behaviour is shown for the oversampling case, and we see again that a clear convergence is obtained. For this case, we use 40 snapshot basis functions per coarse grid block giving a total DOF of 10240, and the corresponding snapshot errors (that is, the difference between the solution obtained by these 10240 basis functions and the solution u_h) of 4.5195×10^{-4} and 9.8935×10^{-4} in relative L^2 norm and relative a-norm respectively. In addition, we observe that the oversampling basis provides more efficient representation of the solution than the non-oversampling basis. To further demonstrate the efficiency of our algorithm, we compare our result with the uniform enrichment scheme. The convergence history for using uniform enrichment is shown in Table 3, and we see that our adaptive enrichment algorithm performs much better than uniform enrichment. Finally, a comparison among all the above cases and the enrichment by exact error is shown in Figure 2, in which the energy error is plotted against DOF. From the figure, we clearly see that our enrichment algorithm performs much better than uniform enrichment. Moreover, our enrichment algorithm performs equally well compared with enrichment by the exact error. This shows that our indicator is both reliable and efficient.

DOF	e_2	e_a
1024	0.1082	0.0479
1769	0.0456	0.0178
2403	0.0156	0.0105
3135	0.0070	0.0067
5607	0.0016	0.0031

DOF	e_2	e_a
1024	0.1082	0.0479
1639	0.0802	0.0239
2584	0.0194	0.0114
3822	0.0061	0.0063
5660	0.0021	0.0037

Table 2: Convergence history with θ=0.4. Left: Enrich in V_1 space only. Right: Enrich in both V_1 and V_2 spaces.

Example 2

In our second example, we will take the source f to be the function shown in the left plot of Figure 3 and the corresponding fine grid solution shown in the right plot of Figure 3. In Table 4 and Table 5, we

DOF	e_2	e_a	e_2^{snap}	e_a^{snap}
1024	0.0940	0.0469	0.0939	0.0469
1975	0.0204	0.0121	0.0202	0.0121
2648	0.0087	0.0077	0.0084	0.0077
3422	0.0046	0.0056	0.0043	0.0056
6748	0.0009	0.0022	0.0006	0.0020

DOF	e_2	e_a
1024	0.1082	0.0479
2048	0.0671	0.0199
3328	0.0423	0.0150
5888	0.0161	0.0059
8448	0.0128	0.0044

Table 3: Left: Convergence history for oversampling basis with $\theta = 0.4$ and enrichment in V_1 space only. Right: Convergence history for uniform enrichment in V_1 space only.

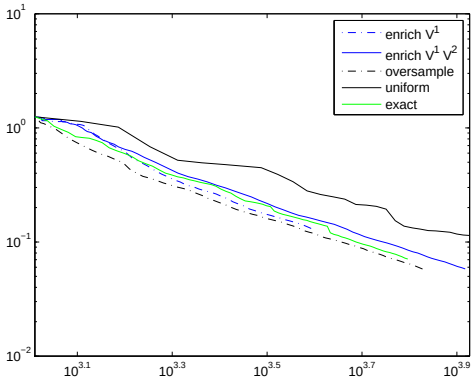

Figure 2: A comparison of different ways of enrichment.

present the convergence history of our algorithm for enriching in V_1 space only, enriching in both V_1 and V_2 spaces and enriching by oversampling basis. We see from Table 4 that enrichment in both V_1 and V_2 spaces provides much more efficient methods than enrichment in V_1 space only. In particular, for an error level of approximately 1%, we see that enrichment in both V_1 and V_2 spaces requires 3144 DOF while enrichment in V_1 space only requires 3483 DOF. In Table 5, the convergence behaviour is shown for the oversampling case, and we see again that a clear convergence is obtained. For this case, we use 40 snapshot basis functions per coarse grid block giving a total DOF of 10240, and the corresponding snapshot errors (that is, the difference between the solution obtained by these 10240 basis functions and the solution u_h) of 0.0078 and 0.0093 in relative L^2 norm and relative a-norm respectively. In addition, we observe again that the oversampling basis provides more efficient representation of the solution than the non-oversampling basis. To further demonstrate the efficiency of our algorithm, we compare our results with the uniform enrichment scheme. The result for using uniform enrichment is shown in Table 5 and we clearly observe that our adaptive method is more efficient. Moreover, a comparison of the performance of various strategies is shown in Figure 4, where the errors against DOF are plotted. From the figure, we see that our method is much better than uniform enrichment. Furthermore, enrichment in both V_1 and V_2 spaces has the best performance, which suggests that both V_1 and V_2 spaces are important for more complicated source functions.

5.1 Adaptive enrichment algorithm

5.1.1 Adaptive enrichment algorithm with basis removal

In our adaptive enrichment algorithm, we can add basis functions to the offline space by using the error indicators. However, the addition of the basis functions must follow the ordering of the eigenfunctions. There may be cases that some of the intermediate eigenfunctions are not required in the representation of the solution. Therefore, we propose a numerical strategy to remove basis functions that do not contribute or

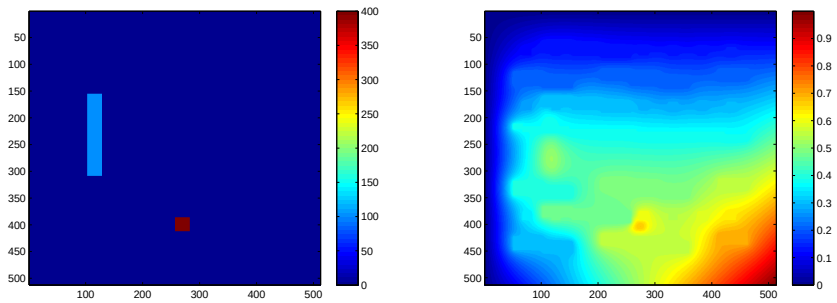

Figure 3: Left: The source function f for the second example. Right: The fine grid solution.

DOF	e_2	e_a
1024	0.2052	0.0554
2028	0.0362	0.0191
2717	0.0152	0.0140
3483	0.0111	0.0118
5116	0.0084	0.0102

DOF	e_2	e_a
1024	0.2052	0.0554
2023	0.0486	0.0206
3144	0.0113	0.0105
4456	0.0050	0.0066
7407	0.0013	0.0034

Table 4: Convergence history with θ=0.4. Left: Enrich in V_1 space only. Right: Enrich in both V_1 and V_2 spaces.

DOF	e_2	e_a	e_2^{snap}	e_a^{snap}
1024	0.1882	0.0540	0.1865	0.0532
1926	0.0296	0.0182	0.0269	0.0156
2626	0.0137	0.0135	0.0098	0.0098
3368	0.0105	0.0116	0.0057	0.0070
6677	0.0080	0.0097	0.0007	0.0025

DOF	e_2	e_a
1024	0.2052	0.0554
2048	0.0923	0.0282
3328	0.0659	0.0215
5888	0.0278	0.0135
8448	0.0226	0.0121

Table 5: Left: Convergence history for oversampling basis with $\theta = 0.4$ and enrichment in V_1 space only. Right: Convergence history for uniform enrichment in V_1 space only.

contribute less to the representation of the solution. In the following, we will present this numerical strategy.

Adaptive enrichment algorithm with basis removal: Choose $0 < \theta < 1$. For each $m = 0, 1, \cdots$,

1. Step 1: Find the solution in the current space. That is, find $u_H^m \in V^{\text{off}}(m)$ such that

$$a_{\text{DG}}(u_H^m, v) = (f, v) \quad \text{for all } v \in V^{\text{off}}(m). \tag{33}$$

2. Step 2: Compute the local residuals. For each coarse grid block K_i, we compute

$$\eta_{j,i}^2 = \|R_{j,i}\|^2 (\lambda^{(i)}_{j,l^m_{j,i}+1})^{-1}, \quad j = 1, 2.$$

   Then we re-enumerate the $2N$ residuals in the decreasing order, that is, $\eta_1^2 \geq \eta_2^2 \geq \cdots \geq \eta_{2N}^2$, where we adopted single index notations.

3. Step 3: Find the coarse grid blocks where enrichment is needed. We choose the smallest integer k such that

$$\theta \sum_{J=1}^{2N} \eta_J^2 \leq \sum_{J=1}^{k} \eta_J^2. \tag{34}$$

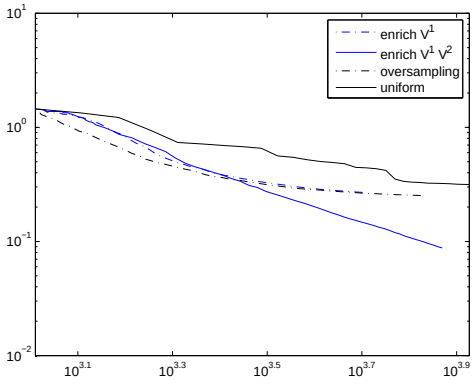

Figure 4: A comparison of different ways of enrichment.

4. Step 4: Enrich the space. For each $J = 1, 2, \cdots, k$, we add basis function in $V_j^{i,\text{off}}$ according to the following rule. Let s be the smallest positive integer such that $\lambda^{(i)}_{j,l^m_{j,i}+s+1}$ is large enough (see the proof of Theorem 4.2) compared with $\lambda^{(i)}_{j,l^m_{j,i}+1}$. Then we include the eigenfunctions in the construction of the basis functions. The resulting space is denoted as $\widehat{V}^{\text{off}}(m+1)$. Note that this is the offline space without basis removal.

5. Step 5: Remove basis. For each coarse grid block K_i, we can write the restriction of the current solution u_H^m on K_i as

$$\sum_{l=1}^{l^m_{1,i}} \alpha_{1,l}\phi_l^{(i)} + \sum_{l=1}^{l^m_{2,i}} \alpha_{2,l}\xi_l^{(i)}.$$

Fixed a tolerance $\varepsilon > 0$. Then the basis function $\phi_l^{(i)}$ or $\xi_l^{(i)}$ is removed if

$$\alpha_{1,l}^2 < \varepsilon\Big(\sum_{l=1}^{l^m_{1,i}} \alpha_{1,l}^2 + \sum_{l=1}^{l^m_{2,i}} \alpha_{2,l}^2\Big) \quad \text{or} \quad \alpha_{2,l}^2 < \varepsilon\Big(\sum_{l=1}^{l^m_{1,i}} \alpha_{1,l}^2 + \sum_{l=1}^{l^m_{2,i}} \alpha_{2,l}^2\Big)$$

is satisfied. The resulting space is called $V^{\text{off}}(m+1)$.

To test this strategy, we consider our second example with the source function f defined in Figure 3. We will consider three choices of ε, with values 10^{-12}, 10^{-13} and 10^{-14}. The convergence history of these cases are shown in Table 6. We can see that our basis removal strategy gives more efficient representation of the solution. For example, comparing the errors with DOF of around 2000 with basis removal (Table 6) and without basis removal (Table 4), we see that the method with basis removal gives a solution with smaller errors in both L^2 norm and a-norm. On the other hand, we see that the choice of $\varepsilon = 10^{-14}$ performs better than $\varepsilon = 10^{-12}$. In particular, for DOF of around 2200, the error with $\varepsilon = 10^{-14}$ is around 2% while the error with $\varepsilon = 10^{-12}$ is around 4%. However, one expects that smaller choices of ε are not as economical as larger choices of ε.

5.1.2 Adaptive enrichment using local basis pursuit

In this section, we discuss an algorithm that follows basis pursuit ideas [4] and identify the basis functions which need to be added based on the residual. The main idea is to find multiscale basis functions that correlate to the residual the most and add those basis functions. More precisely, we identify basis functions

DOF	L_2-error	a-error
1024	0.2052	0.0554
951	0.1824	0.0502
1074	0.1158	0.0415
1742	0.0461	0.0174
2218	0.0404	0.0153

DOF	L_2-error	a-error
1024	0.2052	0.0554
996	0.1767	0.0501
1107	0.1236	0.0431
2006	0.0266	0.0154
2824	0.0192	0.0123

DOF	L_2-error	a-error
1024	0.2052	0.0554
1048	0.1774	0.0500
1185	0.1280	0.0434
2235	0.0223	0.0150
3275	0.0147	0.0117

Table 6: Enrichment with $\theta = 0.4$ and basis removal as well as enrichment in V_1 space only. Left: $\varepsilon = 10^{-12}$. Middle: $\varepsilon = 10^{-13}$. Right: $\varepsilon = 10^{-14}$

that has the largest correlation coefficient with respect to the residual and add those basis functions. In the following, we will present the details of the numerical algorithm.

Adaptive enrichment algorithm using local basis pursuit: Choose $0 < \theta < 1$. For each $m = 0, 1, \cdots,$

1. Step 1: Find the solution in the current space. That is, find $u_H^m \in V^{\text{off}}(m)$ such that
$$a_{\text{DG}}(u_H^m, v) = (f, v) \quad \text{for all } \ v \in V^{\text{off}}(m). \tag{35}$$

2. Step 2: Compute the local residuals. For each coarse grid block K_i, we compute
$$\zeta_{j,i,l}^2 = \frac{|R_{j,i}(v_l)|^2}{\|v_l\|^2_{V_j(K_i)}}, \quad j = 1, 2, \quad \forall v_l \in V_j(K_i).$$
Then we re-enumerate these residuals in the decreasing order, that is, $\zeta_1^2 \geq \zeta_2^2 \geq \cdots$, where we adopted single index notations. Note that $|R_{j,i}(v_l)|$ is the inner-product that identifies the basis functions that have the largest correlation to the residual. More precisely,
$$|R_{j,i}(v_l)| = |\int_{K_i} f v_l - a_{DG}(u_H^m, v_l)|$$
which is just the local inner-product of the residual vector and basis function v_l.

3. Step 3: Find the coarse grid blocks where enrichment is needed. We choose the smallest integer k such that
$$\eta_k \geq \theta \eta_1. \tag{36}$$

4. Step 4: Enrich the space. For each $J = 1, 2, \cdots, k$, we add the basis function $v_l \in V_j(K_i)$ corresponding to ζ_J. The resulting space is denoted as $\widehat{V}^{\text{off}}(m+1)$. Note that this is the offline space without basis removal.

5. Step 5: Remove basis. For each coarse grid block K_i, we can write the restriction of the current solution u_H^m on K_i as
$$\sum_{l=1}^{l_{1,i}^m} \alpha_{1,l} \phi_l^{(i)} + \sum_{l=1}^{l_{2,i}^m} \alpha_{2,l} \xi_l^{(i)}.$$
Fixed a tolerance $\varepsilon > 0$. Then the basis function $\phi_l^{(i)}$ or $\xi_l^{(i)}$ is removed if
$$\alpha_{1,l}^2 < \varepsilon \Big(\sum_{l=1}^{l_{1,i}^m} \alpha_{1,l}^2 + \sum_{l=1}^{l_{2,i}^m} \alpha_{2,l}^2 \Big) \quad \text{or} \quad \alpha_{2,l}^2 < \varepsilon \Big(\sum_{l=1}^{l_{1,i}^m} \alpha_{1,l}^2 + \sum_{l=1}^{l_{2,i}^m} \alpha_{2,l}^2 \Big)$$
is satisfied. The resulting space is called $V^{\text{off}}(m+1)$.

To demonstrate the performance of this strategy, we will consider two examples. In the first example, the source function f is defined as in Figure 3 and the rest of the parameters as in the Example 2. In the second example, we will take the solution (see Figure 5) which only contain the component of the 1st, 17th and 30th eigen-basis. The boundary conditions are as in Example 2 and the source term is calculated based on this sparse solution. The convergence history for the first example is shown in Table 7. Comparing these results to Table 6, we can see that the adaptive enrichment provides a better convergence. The convergence history is substantially improved if we consider the sparse solution as in our second example. The numerical results are shown in Table 8.

DOF	e_2	e_a
1024	0.2052	0.0554
1036	0.1474	0.0405
1259	0.0585	0.0230
2096	0.0129	0.0125
2643	0.0099	0.0111

Table 7: Enrichment using basis pursuit with $\theta = 0.8$ and basis removal as well as enrichment in V_1 space only.

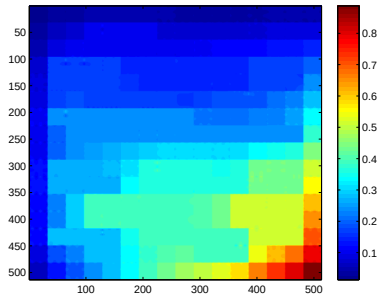

Figure 5: Solution with sparse coefficient

DOF	e_2	e_a
1024	0.0150	0.0424
941	0.0069	0.0286
934	0.0032	0.0135
688	0.0001	0.0010
744	1.20e-06	2.13e-05

DOF	e_2	e_a
1024	0.0150	0.0424
997	0.0150	0.0424
1327	0.0108	0.0412
2447	0.0023	0.0154
889	0.0003	0.0022

Table 8: Enrichment with θ=0.8 . Left: basis pursuit. Right: standard enrichment

6 Convergence analysis

In this section, we will provide the proofs for the a-posteriori error estimates (Theorem 4.1) and the convergence of the adaptive enrichment algorithm (Theorem 4.2).

For each coarse grid block K_i, $i = 1, 2, \cdots, N$, we define two projection operators $P_{j,i} : V_j^{i,\text{snap}} \to V_j^{i,\text{off}}$,

$j = 1, 2$, from the local snapshot spaces to the corresponding local offline spaces by

$$\int_{\partial K_i} \widetilde{\kappa} P_{1,i}(v) w = \int_{\partial K_i} \widetilde{\kappa} v w \qquad \forall w \in V_1^{i,\mathrm{off}},$$
$$\int_{K_i} \kappa P_{2,i}(v) w = \int_{K_i} \kappa v w \qquad \forall w \in V_2^{i,\mathrm{off}}.$$

For any $v \in V_1^{i,\mathrm{snap}}$, we can write $v = \sum_{l=1}^{M_i} c_{1,l} \phi_l^{(i)}$. By orthogonality of eigenfunctions, we have $P_{1,i}(v) = \sum_{l=1}^{l_{1,i}} c_{1,l} \phi_l^{(i)}$. Therefore, by the equivalence of $\|\cdot\|_a$ and $\|\cdot\|_{\mathrm{DG}}$, we have

$$\|P_{1,i}(v)\|_a^2 \leq a_1 \left(\int_{K_i} \kappa |\nabla P_{1,i}(v)|^2 + \frac{\gamma}{h} \int_{\partial K_i} \widetilde{\kappa} P_{1,i}(v)^2 \right).$$

By the spectral problem (6) and the fact that the eigenvalues are ordered increasingly, we have

$$\begin{aligned} \|P_{1,i}(v)\|_a^2 &\leq a_1 \left(\sum_{l=1}^{l_{1,i}} \frac{\lambda_{1,l}^{(i)}}{H} c_{1,l}^2 + \frac{\gamma}{h} \int_{\partial K_i} \widetilde{\kappa} P_{1,i}(v)^2 \right) \\ &\leq a_1 \left(\frac{\lambda_{1,l_{1,i}}^{(i)}}{H} + \frac{\gamma}{h} \right) \sum_{l=1}^{l_{1,i}} c_{1,l}^2 = a_1 \left(\lambda_{1,l_{1,i}}^{(i)} + \frac{\gamma H}{h} \right) \|v\|_{V_1(K_i)}^2. \end{aligned}$$

Similarly, for $v = \sum_{l \geq 1} c_{2,l} \xi_l^{(i)}$, we have $P_{2,i}(v) = \sum_{l=1}^{l_{2,i}} c_{2,l} \xi_l^{(i)}$. Therefore, by the equivalence of $\|\cdot\|_a$ and $\|\cdot\|_{\mathrm{DG}}$, we have

$$\|P_{2,i}(v)\|_a^2 \leq a_1 \left(\int_{K_i} \kappa |\nabla P_{2,i}(v)|^2 \right).$$

By the spectral problem (7) and the fact that the eigenvalues are ordered increasingly, we have

$$\|P_{2,i}(v)\|_a^2 \leq a_1 \left(\sum_{l=1}^{l_{2,i}} \frac{\lambda_{2,l}^{(i)}}{H^2} c_{2,l}^2 \right) \leq a_1 \left(\frac{\lambda_{2,l_{2,i}}^{(i)}}{H^2} \right) \sum_{l=1}^{l_{2,i}} c_{2,l}^2 = a_1 \lambda_{2,l_{2,i}}^{(i)} \|v\|_{V_2(K_i)}^2.$$

Thus the projections $P_{j,i}$ satisfy the following stability bound

$$||P_{j,i}(v)||_a \leq a_1^{\frac{1}{2}} \left(\lambda_{j,l_{j,i}}^{(i)} + \frac{\gamma H}{h} \right)^{\frac{1}{2}} \|v\|_{V_j(K_i)}, \quad j = 1, 2, \quad i = 1, 2, \cdots, N. \tag{37}$$

Next, we will establish some approximation properties for the projection operators $P_{j,i}$. Indeed, by the definitions of the operators $P_{j,i}$, for any $v \in V_j^{i,\mathrm{snap}}$,

$$\|v - P_{j,i}(v)\|_{V_j(K_i)}^2 = H^{-j} \sum_{l \geq l_{j,i}+1} c_{j,l}^2 \leq (\lambda_{l_{j,i}+1}^{(i)})^{-1} \sum_{l \geq l_{j,i}+1} \frac{\lambda_{j,l}^{(i)}}{H^j} c_{j,l}^2 = (\lambda_{j,l_{j,i}+1}^{(i)})^{-1} \int_{K_i} \kappa |\nabla v|^2,$$

and therefore the following convergence result holds

$$\|v - P_{j,i}(v)\|_{V_j(K_i)} \leq \left(\lambda_{j,l_{j,i}+1}^{(i)} \right)^{-\frac{1}{2}} \left(\int_{K_i} \kappa |\nabla v|^2 \right)^{\frac{1}{2}}. \tag{38}$$

For the analysis presented below, we define the projection $\Pi : V^{\mathrm{snap}} \to V^{\mathrm{off}}$ by $\Pi v = \sum_{i=1}^{N} \sum_{j=1}^{2} P_{j,i}(v)$.

6.1 Proof of Theorem 4.1

Let $v \in V_{\mathrm{DG}}^h$ be an arbitrary function in the space V_{DG}^h. Using (23), we have

$$a_{\mathrm{DG}}(u_h - u_H, v) = a_{\mathrm{DG}}(u_h, v) - a_{\mathrm{DG}}(u_H, v) = (f, v) - a_{\mathrm{DG}}(u_H, v).$$

Therefore,

$$a_{\mathrm{DG}}(u_h - u_H, v) = (f, v) - a_{\mathrm{DG}}(u_H, v) = (f, v - \Pi v) + (f, \Pi v) - a_{\mathrm{DG}}(u_H, \Pi v) - a_{\mathrm{DG}}(u_H, v - \Pi v).$$

Thus, using (24), we have

$$a_{\mathrm{DG}}(u_h - u_H, v) = (f, v - \Pi v) - a_{\mathrm{DG}}(u_H, v - \Pi v). \tag{39}$$

Since the space V_{DG}^h is the same as V^{snap}, we can write $v = \sum_{i=1}^{N} \sum_{j=1}^{2} v_j^{(i)}$ with $v_j^{(i)} \in V_j^{i,\mathrm{snap}}$. Hence, (39) becomes

$$a_{\mathrm{DG}}(u_h - u_H, v) = \sum_{i=1}^{N} \sum_{j=1}^{2} \Big(\int_{K_i} f(v_j^{(i)} - P_{j,i} v_j^{(i)}) - a_{\mathrm{DG}}(u_H, v_j^{(i)} - P_{j,i} v_j^{(i)}) \Big). \tag{40}$$

We remark that, in the computation of the term $a_{\mathrm{DG}}(u_H, v_j^{(i)} - P_{j,i} v_j^{(i)})$ in (40), we assume that the second argument is zero outside the coarse grid block K_i.

Using the definition of $R_{j,i}$, we see that (40) can be written as

$$a_{\mathrm{DG}}(u_h - u_H, v) = \sum_{i=1}^{N} \sum_{j=1}^{2} R_{j,i}(v_j^{(i)} - P_{j,i} v_j^{(i)}).$$

Thus, we have

$$a_{\mathrm{DG}}(u_h - u_H, v) \leq \sum_{i=1}^{N} \sum_{j=1}^{2} \|R_{j,i}\| \|(v_j^{(i)} - P_{j,i} v_j^{(i)})\|_{V_j(K_i)}.$$

Using (38),

$$a_{\mathrm{DG}}(u_h - u_H, v) \leq \sum_{i=1}^{N} \sum_{j=1}^{2} \|R_{j,i}\| \Big(\lambda_{j,l_{j,i}+1}^{(i)} \Big)^{-\frac{1}{2}} \Big(\int_{K_i} \kappa |\nabla v_j^{(i)}|^2 \Big)^{\frac{1}{2}}.$$

The inequality (29) is then followed by taking $v = u_h - u_H$ and $\sum_{i=1}^{N} \sum_{j=1}^{2} \int_{K_i} \kappa |\nabla v_j^{(i)}|^2 \leq \|v\|_{\mathrm{DG}}^2 \leq a_0 \|v\|_a^2$.

6.2 An auxiliary lemma

In this section, we will derive an auxiliary lemma which will be used for the proof of the convergence of the adaptive enrichment algorithm stated in Theorem 4.2. We use the notation $P_{j,i}^m$ to denote the projection operator $P_{j,i}$ at the enrichment level m.

In Theorem 4.1, we see that $\|R_{j,i}\|$ gives an upper bound of the energy error $\|u_h - u_H\|_a$. We will first show that, $\|R_{j,i}\|$ is also a lower bound up to a correction term (see Lemma 6.1). To state this precisely, we define

$$S_{j,i}^m = (\lambda_{j,l_{j,i}^m+1}^{(i)})^{-\frac{1}{2}} \sup_{v \in V_j^{i,\mathrm{snap}}} \frac{|R_{j,i}(v - P_{j,i}^m(v))|}{\|v\|_{V_j(K_i)}}. \tag{41}$$

Notice that the residual $R_{j,i}$ is computed using the solution u_H^m obtained at enrichment level m. We omit the index m in $R_{j,i}$ to simplify notations. Next, we will obtain

$$(S_{j,i}^m)^2 = \|R_{j,i}\|^2 (\lambda_{j,l_{j,i}^m+1}^{(i)})^{-1}. \tag{42}$$

Indeed, by the fact that $P_{j,i}^m(v) \in V_j^{i,\text{off}}$,

$$R_{j,i}(P_{j,i}^m(v)) = \int_{K_i} f P_{j,i}^m(v) - a_{\text{DG}}(u_H^m, P_{j,i}^m(v)) = 0.$$

Thus,

$$S_{j,i}^m = (\lambda_{j,l_{j,i}^m+1}^{(i)})^{-\frac{1}{2}} \sup_{v \in V_j^{i,\text{snap}}} \frac{|R_{j,i}(v - P_{j,i}^m(v))|}{\|v\|_{V_j(K_i)}} = (\lambda_{j,l_{j,i}^m+1}^{(i)})^{-\frac{1}{2}} \sup_{v \in V_j^{i,\text{snap}}} \frac{|R_{j,i}(v)|}{\|v\|_{V_j(K_i)}} = (\lambda_{j,l_{j,i}^m+1}^{(i)})^{-\frac{1}{2}} \|R_{j,i}\|.$$

This implies (42).

To prove Theorem 4.2, we will need the following recursive properties for $S_{j,i}^m$ (see Lemma 6.1). Notice that, the notation $\|u\|_{a,K_i}$ is defined as

$$\|u\|_{a,K_i}^2 = a_{\text{DG}}(u,u) = \int_{K_i} \kappa |\nabla u|^2 - \sum_{E \in \partial K_i} 2 \int_E \{\kappa \nabla u \cdot n_E\} [\![u]\!] + \sum_{E \in \partial K_i} \frac{\gamma}{h} \int_E \overline{\kappa} [\![u]\!]^2.$$

Lemma 6.1. *For any $\alpha > 0$, we have*

$$(S_{j,i}^{m+1})^2 \leq (1+\alpha) \frac{\lambda_{j,l_{j,i}^m+1}^{(i)}}{\lambda_{j,l_{j,i}^{m+1}+1}^{(i)}} (S_{j,i}^m)^2 + (1+\alpha^{-1}) a_1 D \|u_H^{m+1} - u_H^m\|_{a,K_i}^2 \tag{43}$$

where the enrichment level dependent constant D is defined by by

$$D = \left(\frac{\Lambda_{j,i}}{\lambda_{j,l_{j,i}^{m+1}+1}^{(i)}} + \frac{\gamma H}{h \lambda_{j,l_{j,i}^{m+1}+1}^{(i)}} \right)$$

with $\Lambda_{j,i} = \max_l \lambda_{j,l}^{(i)}$.

Proof. By direct calculations, we have

$$\begin{aligned}
&\int_{K_i} f(v - P_{j,i}^{m+1}(v)) - a_{\text{DG}}(u_H^{m+1}, v - P_{j,i}^{m+1}(v)) \\
&= \int_{K_i} fv - a_{\text{DG}}(u_H^{m+1}, v) \\
&= \int_{K_i} fv - a_{\text{DG}}(u_H^m, v) + a_{\text{DG}}(u_H^m - u_H^{m+1}, v) \\
&= \int_{K_i} f(v - P_{j,i}^m(v)) - a_{\text{DG}}(u_H^m, v - P_{j,i}^m(v)) + a_{\text{DG}}(u_H^m - u_H^{m+1}, v).
\end{aligned} \tag{44}$$

By definition of $S_{j,i}^m$, we have

$$S_{j,i}^m = (\lambda_{j,l_{j,i}^m+1}^{(i)})^{-\frac{1}{2}} \sup_{v \in V_j^{i,\text{snap}}} \frac{|\int_{K_i} f(v - P_{j,i}^m(v)) - a_{\text{DG}}(u_H^m, v - P_{j,i}^m(v))|}{\|v\|_{V_j(K_i)}}. \tag{45}$$

Multiplying (44) by $(\lambda_{j,l_{j,i}^m+1}^{(i)})^{-\frac{1}{2}} \|v\|_{V_j(K_i)}^{-1}$ and taking supremum with respect to v, we have

$$S_{j,i}^{m+1} \leq \Big(\frac{\lambda_{j,l_{j,i}^m+1}^{(i)}}{\lambda_{j,l_{j,i}^{m+1}+1}^{(i)}} \Big)^{\frac{1}{2}} S_{j,i}^m + I, \tag{46}$$

where

$$I = (\lambda^{(i)}_{j,l^m_{j,i}+1})^{-\frac{1}{2}} \sup_{v\in V_j^{i,\mathrm{snap}}} \frac{|a_{\mathrm{DG}}(u_H^m - u_H^{m+1}, v)|}{\|v\|_{V_j(K_i)}}.$$

To estimate I, we note that

$$a_{\mathrm{DG}}(u_H^m, P^m_{j,i}(v)) = \int_{K_i} f P^m_{j,i}(v) = a_{\mathrm{DG}}(u_H^{m+1}, P^m_{j,i}(v)).$$

Therefore, we have

$$a_{\mathrm{DG}}(u_H^m - u_H^{m+1}, v) = a_{\mathrm{DG}}(u_H^m - u_H^{m+1}, v - P^m_{j,i}(v)) \leq \|u_H^m - u_H^{m+1}\|_{a,K_i}\|v - P^m_{j,i}(v)\|_{a,K_i},$$

where we remark that v has value zero outside K_i. By the stability bound (37),

$$\|v - P^m_{j,i}(v)\|_a \leq a_1^{\frac{1}{2}} \left(\Lambda_{j,i} + \frac{\gamma H}{h}\right)^{\frac{1}{2}} \|v - P^m_{j,i}(v)\|_{V_j(K_i)} \leq a_1^{\frac{1}{2}} \left(\Lambda_{j,i} + \frac{\gamma H}{h}\right)^{\frac{1}{2}} \|v\|_{V_j(K_i)}.$$

Thus we have

$$I \leq a_1^{\frac{1}{2}} (\lambda^{(i)}_{j,l^m_{j,i}+1})^{-\frac{1}{2}} \left(\Lambda_{j,i} + \frac{\gamma H}{h}\right)^{\frac{1}{2}} \|u_H^{m+1} - u_H^m\|_{a,K_i}.$$

Using (46), we get

$$S^{m+1}_{j,i} \leq \Big(\frac{\lambda^{(i)}_{j,l^m_{j,i}+1}}{\lambda^{(i)}_{j,l^{m+1}_{j,i}+1}}\Big)^{\frac{1}{2}} S^m_{j,i} + a_1^{\frac{1}{2}} \left(\frac{\Lambda_{j,i}}{\lambda^{(i)}_{j,l^{m+1}_{j,i}+1}} + \frac{\gamma H}{h\lambda^{(i)}_{j,l^{m+1}_{j,i}+1}}\right)^{\frac{1}{2}} \|u^{m+1}_{\mathrm{ms}} - u^m_{\mathrm{ms}}\|_{a,K_i}.$$

Hence, (43) is proved. □

6.3 Proof of Theorem 4.2

In this section, we prove the convergence of the adaptive enrichment algorithm. First of all, we recall that

$$\eta^2_{j,i} = \|R_{j,i}\|^2 (\lambda^{(i)}_{j,l^m_{j,i}+1})^{-1} = (S^m_{j,i})^2. \tag{47}$$

We will use the single index notation η_J and S^m_J for $\eta_{j,i}$ and $S^m_{j,i}$ respectively.

Let $0 < \theta < 1$. We choose an index set I so that

$$\theta^2 \sum_{J=1}^{2N} \eta^2_J \leq \sum_{J\in I} \eta^2_J. \tag{48}$$

We will then add basis function from $V_j^{i,\mathrm{snap}}$ with $J \in I$. Then, using Theorem 4.1 and (48), we have

$$\theta^2 \|u_h - u_H^m\|^2_a \leq \theta^2 C_{\mathrm{err}} \sum_{J=1}^{2N} \eta^2_J \leq C_{\mathrm{err}} \sum_{J\in I} \eta^2_J.$$

By (47), we also have

$$\|u_h - u_H^m\|^2_a \leq \frac{C_{\mathrm{err}}}{\theta^2} \sum_{J\in I} (S^m_J)^2. \tag{49}$$

On the other hand,

$$\sum_{J=1}^{N}(S_J^{m+1})^2=\sum_{J\in I}(S_J^{m+1})^2+\sum_{J\notin I}(S_J^{m+1})^2.$$

By lemma 6.1, we have

$$\begin{aligned}\sum_{J=1}^{N}(S_J^{m+1})^2 &\leq \sum_{J\in I}\Big((1+\alpha)\frac{\lambda^{(i)}_{j,l^m_{j,i}+1}}{\lambda^{(i)}_{j,l^{m+1}_{j,i}+1}}(S_J^m)^2+(1+\alpha^{-1})a_1D\|u_H^{m+1}-u_H^m\|^2_{a,K_i}\Big)\\ &\quad+\sum_{J\notin I}\left((1+\alpha)(S_J^m)^2+(1+\alpha^{-1})a_1D\|u_H^{m+1}-u_H^m\|^2_{a,K_i}\right).\end{aligned}$$

We assume the enrichment is obtained so that

$$\delta:=\max_{J\in I}\frac{\lambda^{(i)}_{j,l^m_{j,i}+1}}{\lambda^{(i)}_{j,l^{m+1}_{j,i}+1}}\leq\delta_0<1,$$

where δ_0 is independent of m. We then have

$$\sum_{J=1}^{2N}(S_J^{m+1})^2\leq(1+\alpha)\sum_{J=1}^{2N}(S_J^m)^2-(1+\alpha)(1-\delta_0)\sum_{J\in I}(S_J^m)^2+\delta L\|u_H^{m+1}-u_H^m\|_a^2,$$

where

$$L_{m+1}=N_E(1+\alpha^{-1})a_1\Big(\max_{1\leq i\leq N}\max_{1\leq j\leq 2}D\Big),\tag{50}$$

where N_E is the maximum number of edges of coarse grid blocks, and we also emphasise that L_{m+1} depends on m. By (48),

$$\sum_{J=1}^{2N}(S_J^{m+1})^2\leq(1+\alpha)\sum_{J=1}^{2N}(S_J^m)^2-(1+\alpha)(1-\delta_0)\theta^2\sum_{J=1}^{2N}(S_J^m)^2+\delta L_{m+1}\|u_H^{m+1}-u_H^m\|_a^2.$$

Let $\rho=(1+\alpha)(1-(1-\delta_0)\theta^2)$. We choose $\alpha>0$ small enough so that $0<\rho<1$. The above is then written as

$$\sum_{J=1}^{2N}(S_J^{m+1})^2\leq\rho\sum_{J=1}^{2N}(S_J^m)^2+\delta L_{m+1}\|u_H^{m+1}-u_H^m\|_a^2.\tag{51}$$

Note that, by Galerkin orthogonality, we have

$$\|u_H^{m+1}-u_H^m\|_a^2=\|u_h-u_H^m\|_a^2-\|u_h-u_H^{m+1}\|_a^2.$$

So, we have

$$\sum_{J=1}^{2N}(S_J^{m+1})^2\leq\rho\sum_{J=1}^{2N}(S_J^m)^2+\delta L_{m+1}(\|u_h-u_H^m\|_a^2-\|u_h-u_H^{m+1}\|_a^2)\tag{52}$$

which implies

$$\|u_h-u_H^{m+1}\|_a^2+\frac{1}{\delta L_{m+1}}\sum_{J=1}^{2N}(S_J^{m+1})^2\leq\|u_h-u_H^m\|_a^2+\frac{\rho}{\delta L_{m+1}}\sum_{J=1}^{2N}(S_J^m)^2.\tag{53}$$

Finally, using (49),

$$\|u_h-u_H^{m+1}\|_a^2+\frac{1}{\delta L_{m+1}}\sum_{J=1}^{2N}(S_J^m)^2\leq(1-\beta)\|u_h-u_H^m\|_a^2+(\frac{\beta C_{err}}{\theta^2}+\frac{\rho}{\delta L_{m+1}})\sum_{J=1}^{2N}(S_J^m)^2.$$

Let $\beta = \dfrac{\theta^2(1-\rho L_m/L_{m+1})}{\theta^2 + C_{\rm err}\delta L_m}$ and combining the above with (53), we obtain

$$\|u - u_{\rm h}^{m+1}\|_a^2 + \frac{1}{\delta L_{m+1}}\sum_{J=1}^{2N}(S_J^{m+1})^2 \leq (1-\beta)\|u - u_{\rm h}^m\|_a^2 + \frac{(1-\beta)}{\delta L_m}\sum_{J=1}^{2N}(S_J^m)^2. \tag{54}$$

Hence, Theorem 4.2 is proved.

References

[1] Assyr Abdulle and Yun Bai. Adaptive reduced basis finite element heterogeneous multiscale method. *Comput. Methods Appl. Mech. Engrg.*, 257:203–220, 2013.

[2] T. Arbogast. Analysis of a two-scale, locally conservative subgrid upscaling for elliptic problems. *SIAM J. Numer. Anal.*, 42(2):576–598 (electronic), 2004.

[3] S. Brenner and L. Scott. *The Mathematical Theory of Finite Element Methods*. Springer-Verlag, New York, 2007.

[4] Scott Shaobing Chen, David L. Donoho, and Michael A. Saunders. Atomic decomposition by basis pursuit. *SIAM Rev.*, 43(1):129–159, 2001. Reprinted from SIAM J. Sci. Comput. **2**0 (1998), no. 1, 33–61 (electronic) [MR1639094 (99h:94013)].

[5] C.-C. Chu, I. G. Graham, and T.-Y. Hou. A new multiscale finite element method for high-contrast elliptic interface problems. *Math. Comp.*, 79(272):1915–1955, 2010.

[6] E. Chung and Y. Efendiev. Reduced-contrast approximations for high-contrast multiscale flow problems. *Multiscale Model. Simul.*, 8:1128–1153, 2010.

[7] E. Chung, Y. Efendiev, and R. Gibson. An energy-conserving discontinuous multiscale finite element method for the wave equation in heterogeneous media. *Advances in Adaptive Data Analysis*, 3:251–268, 2011.

[8] E. Chung, Y. Efendiev, and W. T. Leung. Generalized multiscale finite element method for wave propagation in heterogeneous media. *arXiv:1307.0123*.

[9] E. Chung, Y. Efendiev, and G. Li. An adaptive GMsFEM for high contrast flow problems. *J. Comput. Phys.*, 273:54–76, 2014.

[10] E. Chung and W. T. Leung. A sub-grid structure enhanced discontinuous galerkin method for multiscale diffusion and convection-diffusion problems. *Commun. Comput. Phys.*, 14:370–392, 2013.

[11] W. Dorfler. A convergent adaptive algorithm for poisson's equation. *SIAM J.Numer. Anal.*, 33:1106 – 1124, 1996.

[12] Martin Drohmann, Bernard Haasdonk, and Mario Ohlberger. Reduced basis approximation for nonlinear parametrized evolution equations based on empirical operator interpolation. *SIAM J. Sci. Comput.*, 34(2):A937–A969, 2012.

[13] L.J. Durlofsky. Numerical calculation of equivalent grid block permeability tensors for heterogeneous porous media. *Water Resour. Res.*, 27:699–708, 1991.

[14] W. E and B. Engquist. Heterogeneous multiscale methods. *Comm. Math. Sci.*, 1(1):87–132, 2003.

[15] Y. Efendiev, J. Galvis, and T. Hou. Generalized multiscale finite element methods. *Journal of Computational Physics*, 251:116–135, 2013.

[16] Y. Efendiev, J. Galvis, R. Lazarov, M. Moon, and M. Sarkis. Generalized multiscale finite element method. Symmetric interior penalty coupling. *J. Comput. Phys.*, 255:1–15, 2013.

[17] Y. Efendiev, J. Galvis, G. Li, and M. Presho. Generalized multiscale finite element methods. oversampling strategies. to appear in International Journal for Multiscale Computational Engineering.

[18] Y. Efendiev, J. Galvis, and X.H. Wu. Multiscale finite element methods for high-contrast problems using local spectral basis functions. *Journal of Computational Physics*, 230:937–955, 2011.

[19] Y. Efendiev and T. Hou. *Multiscale Finite Element Methods: Theory and Applications*, volume 4 of *Surveys and Tutorials in the Applied Mathematical Sciences*. Springer, New York, 2009.

[20] Y. Efendiev, T. Hou, and V. Ginting. Multiscale finite element methods for nonlinear problems and their applications. *Comm. Math. Sci.*, 2:553–589, 2004.

[21] M. Ghommem, M. Presho, V. M. Calo, and Y. Efendiev. Mode decomposition methods for flows in high-contrast porous media. global-local approach. *Journal of Computational Physics, Vol. 253.*, pages 226–238.

[22] T. Hou and X.H. Wu. A multiscale finite element method for elliptic problems in composite materials and porous media. *J. Comput. Phys.*, 134:169–189, 1997.

[23] Dinh Bao Phuong Huynh, David J. Knezevic, and Anthony T. Patera. A static condensation reduced basis element method: approximation and *a posteriori* error estimation. *ESAIM Math. Model. Numer. Anal.*, 47(1):213–251, 2013.

[24] K. Mekchay and R. H. Nochetto. Convergence of adaptive finite element method for general second order elliptic PDEs. *SIAM J. Numer. Anal.*, 43:1803–1827, 2005.

[25] N. C. Nguyen, G. Rozza, D. B. P. Huynh, and A. T. Patera. Reduced basis approximation and a posteriori error estimation for parametrized parabolic PDEs: application to real-time Bayesian parameter estimation. In *Large-scale inverse problems and quantification of uncertainty*, Wiley Ser. Comput. Stat., pages 151–177. Wiley, Chichester, 2011.

[26] Beatrice M. Riviere. *Discontinuous Galerkin Methods For Solving Elliptic And parabolic Equations: Theory and Implementation*. SIAM, 2008.

[27] Timo Tonn, K. Urban, and S. Volkwein. Comparison of the reduced-basis and POD *a posteriori* error estimators for an elliptic linear-quadratic optimal control problem. *Math. Comput. Model. Dyn. Syst.*, 17(4):355–369, 2011.

[28] X.H. Wu, Y. Efendiev, and T.Y. Hou. Analysis of upscaling absolute permeability. *Discrete and Continuous Dynamical Systems, Series B.*, 2:158–204, 2002.